Development of ROV for Visual Inspection of Concrete Pier Superstructure

Toshinari Tanaka, Shuji Nogami, Ema Kato and Tsukasa Kita

Port and Airport Research Institute, National Institute of Maritime, Port and Aviation Technology, Japan
E-mail: tanaka_t@p.mpat.go.jp, nogami-s852a@p.mpat.go.jp, katoh-e@p.mpat.go.jp, kita-t@p.mpat.go.jp

Abstract –

Visual inspections of underside of concrete superstructures of piled piers are usually carried out by inspectors on small boat or divers. it is not easy to ensure work safety in such a narrow space because of affection by waves and tides during inspection work. And, in-service facilities require to carry out the inspection work efficiently within a limited amount time and period. Therefore, the authors developed a ROV type inspection device with various support functions that takes images of the underside of the pier superstructure for improving the safety and efficiency of the inspection work. Moreover, we also developed a software to support documentation of the inspection and diagnosis of pier superstructures.

In this paper, a developed ROV for visual inspection of concrete pier superstructure and cooperation between various support functions are described.

Keywords –

Visual inspection; Concrete pier superstructure; ROV; Work support functions

1 Introduction

In typical periodic inspections, visual inspections of underside of concrete superstructures of piled piers are usually carried out by inspectors on small boat. If there is insufficient clearance to access the underside by boats, divers carry out the inspection work. However, it is not easy to ensure work safety in such a narrow space because it is affected by tidal and wave conditions during work. In addition, inspection work should be carried out efficiently so that it does not interfere with the mooring or cargo works.

For the purpose of improving the safety and efficiency of such inspection work, our R&D group has been developed a ROV (Remotely Operated Vehicle) type inspection device that takes images for diagnosis of the underside of the pier superstructure by remote control from land since 2014. We have been conducting the ROV demonstration tests since 2017, and the ROV was equipped with various work support functions at each development phase in order to reliably navigate and operate the ROV in the environments described above. Typical support functions are a positioning under the pier superstructure without using GNSS (Global Navigation Satellite System), shooting position management, a collision avoidance for obstacles, and a shooting history presentation for preventing shooting omissions. Moreover, we also developed a software for documentation of inspection and diagnosis to support in-house work.

In this paper, a developed ROV for visual inspection of concrete pier superstructure and cooperation between various support functions are described in detail by citing references of each development report.

2 ROV for Visual Inspection of Concrete Pier Superstructure

The ROV for visual inspection of concrete pier superstructure, named ROV-PARI, consists of an underwater vehicle platform and the camera system intended for concreate superstructure shooting. This is a semi-submersible ROV with a camera mounted on the top of the underwater vehicle platform and floats on the side. With this configuration, the distance from the center of buoyancy to the center of gravity can be extended, and so the ROV ensured stability against hull fluctuation.

The underwater vehicle platform is a movable body with payload part and a device extension function. It is equipped with an underwater camera and six underwater propulsor units, and can be also used as a general ROV that can dive up to 200m by itself. The underwater camera of the underwater vehicle platform and the two aerial cameras in front and behind make a wide field of view when operating as ROV-PARI.

The camera system intended for the superstructure shooting is equipped with one GigE camera for preview and image processing and one digital single-lens reflex camera (DSLR) for inspection images facing upward. It is as tolerant to low-light and deposits as humans.

In addition, ROV-PARI is equipped with LRF (Laser Range Finder) in order to grasp the situation of obstacles around itself, and a directional gyro is installed for the

ROV's own heading estimation. The scanning results obtained from the two LRFs are combined to form the omnidirectional scanning result and be imaged, and pier piles are detected by image processing, and its position information are used. The positions of these detected piles and the piles in the map database are collated, the collated piles are regarded as landmarks, and the ROV's own position and heading seen from the position of the landmarks are estimated by inverse calculation. In the case that the number of collated piles is less than two, the ROV's own heading is estimated by the directional gyro. Moreover, the ROV's own position and direction are measured using a GPS compass on the sea outside piers.

Therefore, attaching the position information to the obtained pictures, it is possible to manage the inspection position. Figure 1 shows ROV-PARI, and Table 1 shows the specifications.

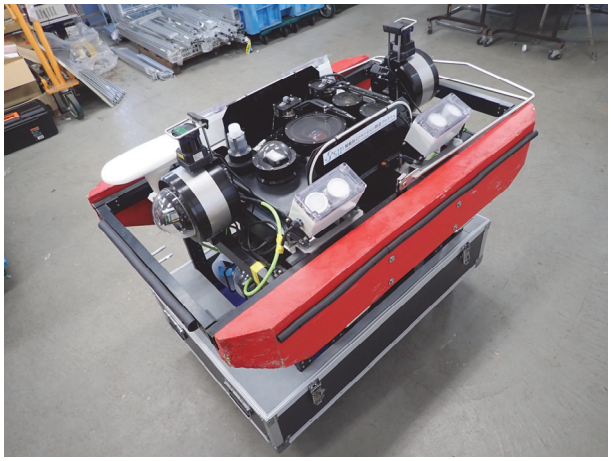

a) ROV-PARI

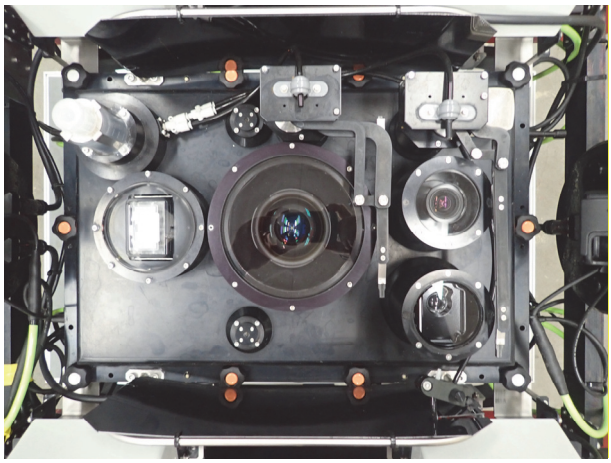

b) Camera system with glass surface cleaning function

Figure 1. The ROV for visual inspection of concrete pier superstructure

Table 1. Specifications of ROV-PARI (2019)

Items	Specifications
Cameras	<u>For navigation</u> GigE* camera with pan, tilt, AF and zoom×1 in-water (forward) GigE* cameras with pan, tilt, AF and zoom×2 in-air (forward and backward)
	<u>For inspection</u> GigE* camera×1 (f=3.5) for preview and image processing Full-size DSLR** camera (f=14mm)×1
Lights	Forward Dimmable LED 1W×12 Upward LED with 80deg diffuser×8
Sensors	<u>On ROV platform</u> Pressure gauge×1 Direction sensor×1 (magnetic compass + MEMS gyroscope)
	<u>On upward camera system</u> Laser Distance meter×1 Laser marker×1 (2pts, W=250mm) LRF***×2 (270deg) Directional gyroscope (FOG****)×1 GPS compass×1
Thrusters	Forward and side thrusters 200W×4 Vertical thrusters 200W×2
Performance	Maximum speed: about 1.5kts
Other functions	Direction keeping, Depth keeping (ROV platform only) Power outlet×8 (selected from DC5V50W, 12V100W, 24V400W) Universal I/O port×8 (selected from LAN 1000BASE-T, RS232C) Autonomous collision avoidance Positioning under slabs using LRFs
Dimension	L1200×W800×H925 except lugs
Mass	About 100kg without ballasts and optional devices

*GigE; Gigabit Ethernet
**DSLR; Digital Single-lens Reflex
***LRF; Laser Range Finder
****FOG; Fiber Optic Gyro

Figure 2 shows usage situations of the ROV equipped with tele-operation assistance functions. a) shows lifting recovery of the ROV using cage without rigging, and b) shows situation of the ROV operation by onshore equipment.

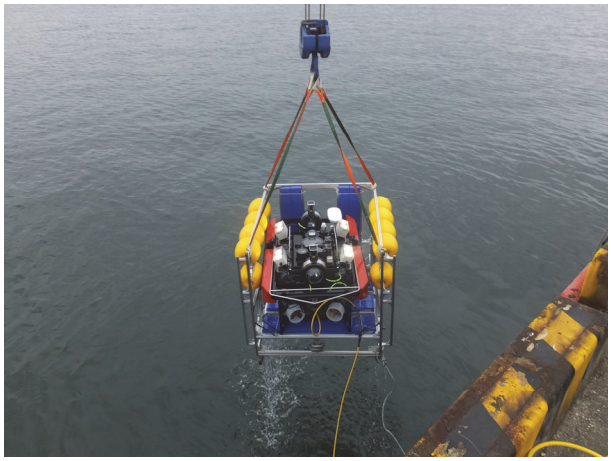

a) Lifting recovery of ROV-PARI using cage without rigging

b) Situation of ROV-PARI operation by onshore equipment

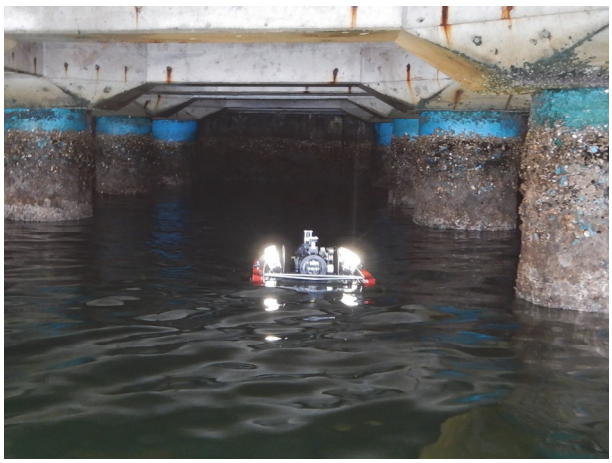

c) Automatic shooting underside of pier superstructure

Figure 2. Usage situations of ROV-PARI

3 Work Support Functions

3.1 Software for In-situ the ROV-PARI Operation

The ROV is remotely operated while confirming the shooting position on the software for in-situ ROV-PARI operation onshore. Figure 3 shows the screenshot of the software used by operators.

In order to support the operation and navigation of the ROV by the operator, the software presents the ROV position information and surrounding obstacles information in real time. This figure is a screenshot while actual operation in the field verification test. Operation panels are prepared on the left side of the window, and various support functions can be used by checking the necessary functions. The main functions are described below:

- CamConPanel: Shooting interval setting. Checking “HIGH” is 1 second, and “MIDDLE” is 2 seconds.
- INSTRUMENTS: Power control of each of the following devices: “CAMERA (all upward cameras)”, “O-GYRO (optical-gyro)”, “LRF (Lase Range Finder)”, “DISTANCE (distance meter)”. LRFs and distance meter are indispensable devices for making after-mentioned “COLLISION AVOIDANCE” and “FOOT PRINT” work.
- GPS COMPASS: Checking “GPS”, it is possible to measure the position and heading of the ROV on the sea outside piers. Mainly used for initial position setting before approaching under pier.
- A-CAS: Autonomous Collision Avoidance System. Measuring positional relationship with obstacles detected by LRFs, the ROV avoids collision with obstacles autonomously. The avoidance action is added to human operation. Checking “UP LINK”, onshore equipment and the ROV are connected. Checking “COLLISION AVOIDANCE”, the function is working.
- REC: Recording logs. Checking “REC LOG”, log recording and interval shooting are started.
- SHOOTIN: Shooting functions. Blue line rectangle is shooting area calculated by shooting distance and optical system of camera, and fill the shoot area. Checking “FOOT PRINT”, shooting history is presented. On “ERASE EP” button down, shooting history is reset. On “ONE SHOT” button down, one picture is shoot manually.

On the lower left side of the screen, an image of the underside of the pier superstructure taken by the GigE camera for preview described in Chapter 2 among the two upper cameras installed is constantly displayed. This shooting area is slightly narrower than the area of DSLR for inspection images.

On the lower right side of the screen, the all-around scanning image obtained by LRFs is displayed. Namely, measuring the relative positional relationship with surrounding objects and obstacles obtained by all-around scanning is calculated, and the result is always displayed in heading-up. Using the relative position information of the closest and second closet piles, shown in Figure 3 as pink and orange piles respectively, the position of the ROV is estimated from the relative position with the closest pile, and the heading is estimated from the angle between the line segment of the closest-the second closet piles and the ROV itself. The positioning function is described in Section 3.2.

In addition, since the all-around scanning result using LRFs are obtained while the positioning process, not only the piles but also the surrounding obstacles are observed. The collision avoidance direction and the level are presented by measuring the relative positional relationship with surrounding objects, and the autonomous collision avoidance behaviour is performed based on this information. The autonomous collision avoidance function is described in Section 3.3.

On the top of the screen is a map created from the prepared pile placement information. By displaying the ROV on this map based on the previous positioning result, the operator can grasp the current position of the ROV under the pier superstructure, and the reliable operation of the ROV along the pre-planned inspection route is possible. Blue line rectangle is shooting area, and filled it is presented as shooting history. In the figure, the filled area in light grey is the captured area. It is possible to easily distinguish captured area and the uncaptured area underside of the pier superstructure in real time, and toto present the omission of shooting. The shooting history presentation is described in Section 3.4.

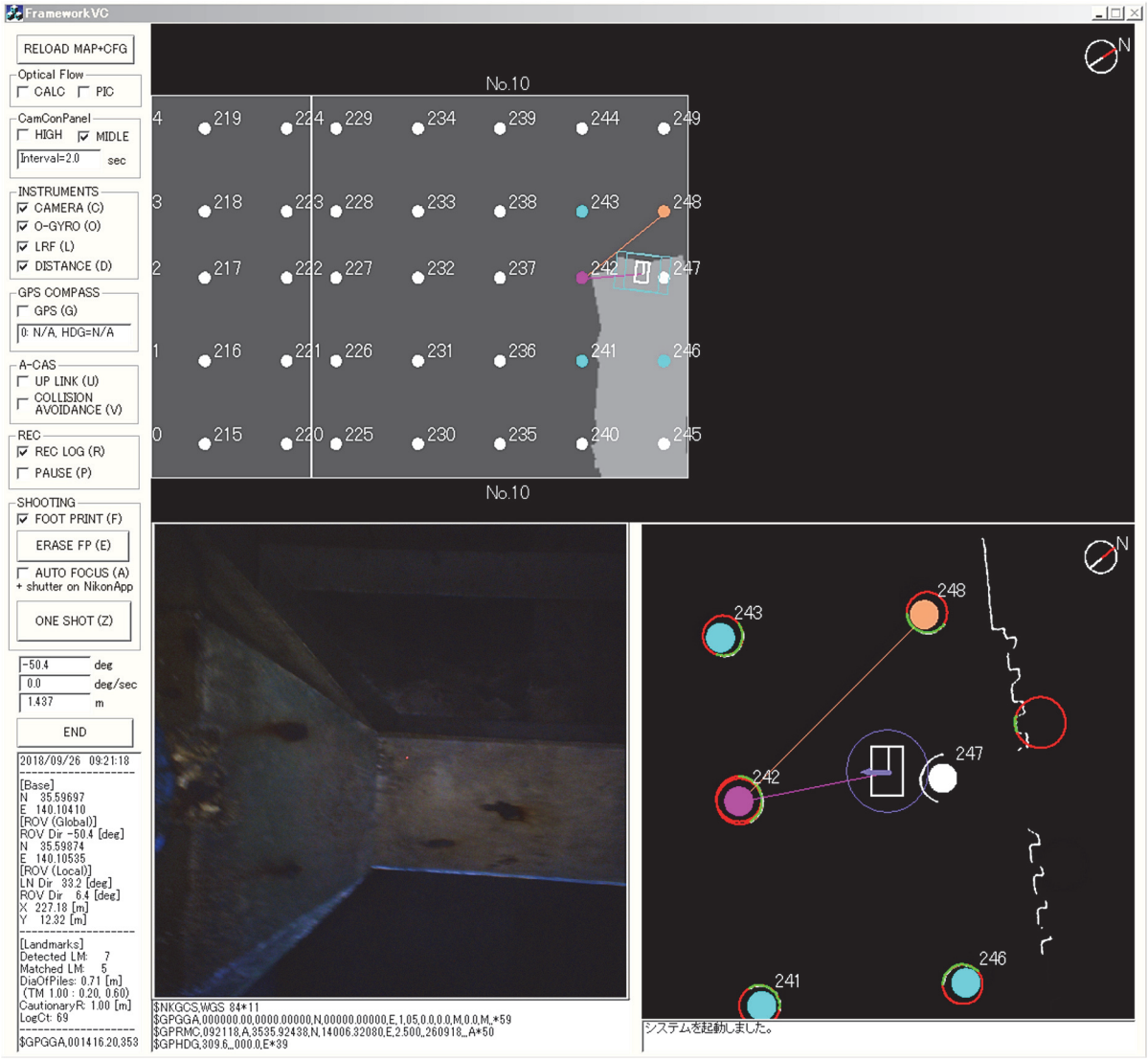

Figure 3. Screenshot of software for in-situ ROV-PARI operation

3.2 Positioning under Pier Superstructures

First, the scanning results obtained by the two LRFs are combined to make an all-around scanning result and is imaged. Next, the piles are detected from the image by image processing, and the position information are used. In fact, the positions of these detected piles and the piles in the map database are collated, the collated piles are regarded as landmarks, and the ROV's own position and heading seen from the position of the landmarks are estimated by inverse calculation.

When there are two or more Matched piles that succeeded in matching the position of the "detected objects" of circular cross-sectional shape by image processing from the scanning image with the position of the piles in the map database, the matched pile proximate to the ROV is "reference point for positioning" (Pink circle in Figure 3) and positioning of the ROV's own position is conducted relative to the point (Pink line in Figure 3). Next, the matched pile secondly proximate to the ROV is the "auxiliary point for azimuth estimation"(Orange circle in Figure 3.), and the heading of the ROV is estimated from the angle between the baseline connecting the positioning reference point and the azimuth estimation auxiliary point (Orange line in Figure 3) and the ROV. In case that the number of matched piles is less than one, the heading estimation is switched to the gyro-base. In case that there is no matched pile, the position estimation of the ROV is allowed to be switched to inertial navigation.

The mathematical presentations of the positioning are shown in the following sections. The first and second axes of the ROV coordinate system are the Roll and Pitch axes on the horizontal plane, and the third axis is the vertically downward Yaw axis, respectively.

The first and second axes of the local map coordinate system are the axis parallel to the face line of the wharf and the orthogonal axis that land side is positive on the horizontal plane, and the third axis is vertically upward, respectively. The first and second axes of the world coordinate system are north latitude and east longitude, and the third axis is vertically downward, respectively. However, all coordinate systems are positive-oriented.

3.2.1 Position on a Local Map Coordinate System

Each positional vector of the piles is defined in Equation (1). Here, the left-superscripts of the variables represent the coordinate systems, and the right-subscripts of the variables represent the objects. Bolds represent vectors or matrices.

$$
\begin{aligned}
&{}^{\mathrm{ROV}}\boldsymbol{P}_{\mathrm{MAP}_k},\ {}^{\mathrm{MAP}}\boldsymbol{P}_{\mathrm{MAP}_k} &&: \text{Piles positions}\\
&{}^{\mathrm{ROV}}\boldsymbol{P}_{\mathrm{RES}_j},\ {}^{\mathrm{MAP}}\boldsymbol{P}_{\mathrm{RES}_j} &&: \text{DP positions}\\
&{}^{\mathrm{ROV}}\boldsymbol{P}_{\mathrm{RES}_{P_i}},\ {}^{\mathrm{MAP}}\boldsymbol{P}_{\mathrm{RES}_{P_i}} &&: \text{MP positions}\\
&{}^{\mathrm{ROV}}\boldsymbol{P}_{\mathrm{MAP}_{Q_i}},\ {}^{\mathrm{MAP}}\boldsymbol{P}_{\mathrm{MAP}_{Q_i}} &&: \text{MP positoin on the local map}
\end{aligned}
\tag{1}
$$

Here, the position of the detected pile j is compared with that of the pile k on the map database, and if the norm between them is less than or equal to a threshold, the detected pile j is regarded as the pile k, and is becomes the matched pile i. In addition, P_i is an index which sorted i in near order to the ROV, and Q_i is the index corresponding to P_i on the map database. After that, P_1 and Q_1 are the index of the proximate matching piles to the ROV, and regarded as positioning reference points, then P_2 and Q_2 are the index of the secondly proximate matching pile to the ROV, and are regarded as auxiliary points for azimuth estimation. The heading and positional vectors of the ROV are defined in Equation (2).

$$
\begin{aligned}
&{}^{\mathrm{ROV}}\theta_{\mathrm{MAP}}: \text{Angle btween first axes of ROV and MAP}\\
&{}^{\mathrm{MAP}}\theta_{\mathrm{ROV}}: \text{Angle between first axes of MAP and ROV}\\
&{}^{\mathrm{ROV}}\theta_{\mathrm{RES}_{P_1\to P_2}}: \text{Angle between ROV and segment RES}_{P_1\to P_2}\\
&{}^{\mathrm{MAP}}\theta_{\mathrm{MAP}_{Q_1\to Q_2}}: \text{Angle between MAP and segment MAP}_{Q_1\to Q_2}\\
&{}^{\mathrm{ROV}}\boldsymbol{P}_{\mathrm{ROV}},\ {}^{\mathrm{MAP}}\boldsymbol{P}_{\mathrm{ROV}}: \text{Positioal vectors of the ROV}\\
&\boldsymbol{R}_1(\theta): \text{Rotation matrix. The subscript is rotational axis}\\
&\quad \text{, and the argument is rotational angle.}\\
&\text{where,}\quad {}^{\mathrm{ROV}}\boldsymbol{P}_{\mathrm{ROV}} \equiv \boldsymbol{O}
\end{aligned}
\tag{2}
$$

From the above definition, if there are two or more matching piles, heading of the ROV ${}^{\mathrm{MAP}}\theta_{\mathrm{ROV}}$ in the local map coordinate system can be estimated by using the positioning reference point and the auxiliary point for azimuth estimation from Equation (3) [1].

$$
\begin{aligned}
{}^{\mathrm{ROV}}\theta_{\mathrm{RES}_{P_1\to P_2}} &= \operatorname{atan2}\left(\frac{{}^{\mathrm{ROV}}y_{\mathrm{RES}_{P_2}} - {}^{\mathrm{ROV}}y_{\mathrm{RES}_{P_1}}}{{}^{\mathrm{ROV}}x_{\mathrm{RES}_{P_2}} - {}^{\mathrm{ROV}}x_{\mathrm{RES}_{P_1}}}\right)\\
{}^{\mathrm{MAP}}\theta_{\mathrm{MAP}_{Q_1\to Q_2}} &= \operatorname{atan2}\left(\frac{{}^{\mathrm{MAP}}y_{\mathrm{MAP}_{Q_2}} - {}^{\mathrm{MAP}}y_{\mathrm{MAP}_{Q_1}}}{{}^{\mathrm{MAP}}x_{\mathrm{MAP}_{Q_2}} - {}^{\mathrm{MAP}}x_{\mathrm{MAP}_{Q_1}}}\right)\\
{}^{\mathrm{ROV}}\theta_{\mathrm{MAP}} &= {}^{\mathrm{ROV}}\theta_{\mathrm{RES}_{P_1\to P_2}} - {}^{\mathrm{MAP}}\theta_{\mathrm{MAP}_{Q_1\to Q_2}}\\
{}^{\mathrm{MAP}}\theta_{\mathrm{ROV}} &= {}^{\mathrm{MAP}}\theta_{\mathrm{ROV}_{inc}} = -{}^{\mathrm{ROV}}\theta_{\mathrm{MAP}}
\end{aligned}
\tag{3}
$$

If Equation (3) cannot be used because the number of matched piles is less than 1, it is possible to seamlessly switch the heading source from Equation (3) to ${}^{\mathrm{MAP}}\theta_{\mathrm{ROV}_{inc}}$ and to estimate ${}^{\mathrm{MAP}}\theta_{\mathrm{ROV}}$ by initializing the heading ${}^{\mathrm{MAP}}\theta_{\mathrm{ROV}_{inc}}$ by the directional gyro with ${}^{\mathrm{ROV}}\theta_{\mathrm{MAP}}$ while the heading ${}^{\mathrm{ROV}}\theta_{\mathrm{MAP}}$ can be estimated by Equation (3).

Next, the relative positioning method of the ROV position in the local map coordinate system is described. Here, the ROV position vector ${}^{\mathrm{MAP}}\boldsymbol{P}_{\mathrm{ROV}}$ in the local map coordinate system is calculated by Equation (4) using the estimated heading and the positional vector of the positioning reference point.

$$
\begin{aligned}
\begin{pmatrix} {}^{\mathrm{MAP}}\boldsymbol{P}_{\mathrm{ROV}} \\ 1 \end{pmatrix} &= \begin{pmatrix} \boldsymbol{R}_3\left({}^{\mathrm{MAP}}\theta_{\mathrm{ROV}}\right) & {}^{\mathrm{MAP}}\boldsymbol{P}_{\mathrm{MAP}_{Q_1}} \\ \boldsymbol{O}^T & 1 \end{pmatrix} \begin{pmatrix} -{}^{\mathrm{ROV}}\boldsymbol{P}_{\mathrm{RES}_{P_1}} \\ 1 \end{pmatrix}\\
{}^{\mathrm{MAP}}\boldsymbol{P}_{\mathrm{ROV}} &= \boldsymbol{R}_3\left({}^{\mathrm{MAP}}\theta_{\mathrm{ROV}}\right)\left(-{}^{\mathrm{ROV}}\boldsymbol{P}_{\mathrm{RES}_{P_1}}\right) + {}^{\mathrm{MAP}}\boldsymbol{P}_{\mathrm{MAP}_{Q_1}}
\end{aligned}
\tag{4}
$$

If the number of matched piles is less than one, the heading estimation is switched to the gyro-base. If there are no matched piles, the positional estimation is allowable to be switched to inertial navigation and so on.

Finally, using the positional vectors and heading of the ROV estimated, the positional vectors of piles on the map database in the ROV coordinate system is updated by Equation (5). As a result, the new detected piles and the new map database can be collated even in the next positioning step, and positioning can be continued.

$$^{\mathrm{ROV}}\boldsymbol{P}_{\mathrm{MAP}_k} = \boldsymbol{R}_3(^{\mathrm{ROV}}\theta_{\mathrm{MAP}})(^{\mathrm{MAP}}\boldsymbol{P}_{\mathrm{MAP}_k} - ^{\mathrm{MAP}}\boldsymbol{P}_{\mathrm{ROV}}) \quad (5)$$

3.2.2 Transform to the World Coordinate System

Positional vector of the origin of the local map coordinate system $^{\mathrm{MAP}}\boldsymbol{P}_{\mathrm{MAP}} \equiv \boldsymbol{O}$ is $^{\mathrm{W}}\boldsymbol{P}_{\mathrm{MAP}}$ in world coordinate system, and the inclination of the local map coordinate system with respect to the world coordinate system is direction of face line of the wharf $^{\mathrm{W}}\theta_{\mathrm{MAP}}$. Transformation to world coordinate system of $^{\mathrm{MAP}}\boldsymbol{P}_{\mathrm{ROV}}$ estimated by Equation (4) is represented by rotation trough $^{\mathrm{W}}\theta_{\mathrm{MAP}}$ about third axis, multiplying by meter-lat/long transformation matrix $\boldsymbol{L}$, and parallel translation $^{\mathrm{W}}\boldsymbol{P}_{\mathrm{MAP}}$ [1].

The equation for conversion the positional vector of the ROV $^{\mathrm{MAP}}\boldsymbol{P}_{\mathrm{ROV}}$ in the local map coordinate system to world coordinate system is shown in Equation (6).

$$\begin{pmatrix} ^{\mathrm{W}}\boldsymbol{P}_{\mathrm{ROV}} \\ 1 \end{pmatrix} = \begin{pmatrix} \boldsymbol{L} & \boldsymbol{O} \\ \boldsymbol{O}^T & 1 \end{pmatrix} \begin{pmatrix} \boldsymbol{R}_3(^{\mathrm{W}}\theta_{\mathrm{MAP}}) & ^{\mathrm{W}}\boldsymbol{P}_{\mathrm{MAP}} \\ \boldsymbol{O}^T & 1 \end{pmatrix} \begin{pmatrix} \boldsymbol{R}_1(\pi) \cdot ^{\mathrm{MAP}}\boldsymbol{P}_{\mathrm{ROV}} \\ 1 \end{pmatrix}$$
$$^{\mathrm{W}}\boldsymbol{P}_{\mathrm{ROV}} = \boldsymbol{L} \cdot \boldsymbol{R}_3(^{\mathrm{W}}\theta_{\mathrm{MAP}})(\boldsymbol{R}_1(\pi) \cdot ^{\mathrm{MAP}}\boldsymbol{P}_{\mathrm{ROV}}) + ^{\mathrm{W}}\boldsymbol{P}_{\mathrm{MAP}} \quad (6)$$

According to the Chronological Scientific Tables (NAOJ), the length $\Delta l_{\mathrm{LAT}}[\mathrm{m/deg}]$ corresponding to a latitude of 1deg depending on the geographical latitude φ and the length $\Delta l_{\mathrm{LON}}[\mathrm{m/deg}]$ corresponding to a longitude of 1deg are approximately expressed by the Equation (7).

Therefore, the meter-lat/long transformation matrix $\boldsymbol{L}$ around geographical latitude φ and in the vicinity of $^{\mathrm{W}}\boldsymbol{P}_{\mathrm{MAP}}$ is given by Equation (8). If GRS 80 is applied as an earth ellipsoid model, the equatorial radius a is 6 378 137m, and the ellipticity f is 1/298.257 222 101. Moreover, the eccentricity of the earth ellipsoid e is $\sqrt{f(2-f)}$, and e^2 is an approximate value of 0.006 694 380 022 900 788.

$$\Delta l_{\mathrm{LAT}} \approx {}^{\pi}/_{180} \cdot {}^{a(1-e^2)}/_{(1-e^2\sin^2\varphi)^{3/2}}$$
$$\Delta l_{\mathrm{LON}} \approx {}^{\pi}/_{180} \cdot {}^{a\cos\varphi}/_{\sqrt{1-e^2\sin^2\varphi}} \quad (7)$$

$$\boldsymbol{L} = \begin{pmatrix} 1/\Delta l_{\mathrm{LAT}} & 0 & 0 \\ 0 & 1/\Delta l_{\mathrm{LON}} & 0 \\ 0 & 0 & 1 \end{pmatrix} \quad (8)$$

3.2.3 Correspondence between Shooting Position Information and Obtained Pictures

Two methods are prepared regarding the correspondence between the obtained pictures and the shooting-attribute information such as shooting position. One is directly attaching to the picture data on real-time and another one is recording in a log file synchronized with the shooting time.

The first method is to convert the latitude and longitude position information in world coordinate system calculated by Equation (6) into NMEA0183-compliant packet information and pass it directly to the camera at the same time as shooting. The shooting date and time, shooting direction, shooting position, and so on are directly written in the Exif GPS IFD tag in the picture data, then it is possible integrally to manage and to utilize the obtained pictures in conjunction with shooting position on a map-linked photo viewer or GIS application.

The second method is to prepare a log file synchronized with the shooting, and record the shooting date and time, shooting direction, shooting position, and so on at the same time of shooting in the file. Here, in addition to the latitude and longitude position information in world coordinate system recorded of the first method, the position information in the local map coordinate system with higher resolution calculated by Equation (4) is also recorded. it is possible to utilize highly accurate position information on the local map coordinate system, and it makes easy to secondary use of obtained pictures using shooting position such as making development view using the obtained pictures.

3.3 Avoidance Direction and Autonomous Collision Avoidance Function

Collision avoidance direction is presented on the operation screen in order to support remote control of the ROV. First, the distance L_{LRF_θ} from the ROV to the first reflection points all-around direction observed by two LRFs are obtained. Next, as shown in Figure 4, an alert circle (broken line) with radius R_{margin} is set around the ROV, the weight w_θ in each direction is calculated by Equation (9) according to the magnitude relationship of L_{LRF_θ} and R_{margin}.

As a result, the avoidance direction vector $^{\mathrm{ROV}}\boldsymbol{A}_{\mathrm{LRF}}$ in the ROV coordinate system is calculated by the Equation (9) according to multiply the unit vector $\boldsymbol{e}_\theta$ of each direction by the weight w_θ and taking the sum [1].

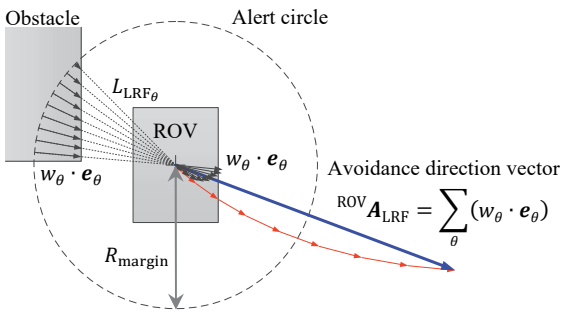

Figure 4. Calculation of collision avoidance direction based on the LRFs

$$
{}^{\mathrm{ROV}}\boldsymbol{A}_{\mathrm{LRF}} = \sum_{\theta}(w_{\theta} \cdot \boldsymbol{e}_{\theta})
$$
$$
\text{where,}\quad w_{\theta} = \begin{cases} -\frac{R_{\mathrm{margin}} - L_{\mathrm{LRF}_{\theta}}}{R_{\mathrm{margin}}} & \left(\text{if } L_{\mathrm{LRF}_{\theta}} \le R_{\mathrm{margin}}\right) \\ 0 & \left(\text{if } L_{\mathrm{LRF}_{\theta}} > R_{\mathrm{margin}}\right) \end{cases} \tag{9}
$$

Here, since the collision avoidance direction is indicated by ${}^{\mathrm{ROV}}\boldsymbol{A}_{\mathrm{LRF}}$, the collision avoidance behaviour vector ${}^{\mathrm{ROV}}\boldsymbol{B}_{\mathrm{LRF}}$ is multiplied by the gain G, and expressed by Equation (10).

$$
{}^{\mathrm{ROV}}\boldsymbol{B}_{\mathrm{LRF}} = G \cdot {}^{\mathrm{ROV}}\boldsymbol{A}_{\mathrm{LRF}} \tag{10}
$$

In addition, the ROV always receives the normalized navigation vector ${}^{\mathrm{ROV}}\boldsymbol{B}_{\mathrm{JOY}}$ by the joystick operation. Therefore, the total navigation vector ${}^{\mathrm{ROV}}\boldsymbol{B}_{\mathrm{TOTAL}}$ of the ROV is expressed by Equation (11) with saturation condition according that the collision avoidance behaviour vector ${}^{\mathrm{ROV}}\boldsymbol{B}_{\mathrm{LRF}}$ is added to the navigation vector ${}^{\mathrm{ROV}}\boldsymbol{B}_{\mathrm{JOY}}$ [2].

$$
{}^{\mathrm{ROV}}\boldsymbol{B}_{\mathrm{TOTAL}} = \begin{cases} {}^{\mathrm{ROV}}\boldsymbol{B}_{\mathrm{JOY}} + {}^{\mathrm{ROV}}\boldsymbol{B}_{\mathrm{LRF}} & \left(\text{if } \left|{}^{\mathrm{ROV}}\boldsymbol{B}_{\mathrm{JOY}} + {}^{\mathrm{ROV}}\boldsymbol{B}_{\mathrm{LRF}}\right| \le 1\right) \\ \frac{{}^{\mathrm{ROV}}\boldsymbol{B}_{\mathrm{JOY}} + {}^{\mathrm{ROV}}\boldsymbol{B}_{\mathrm{LRF}}}{\left|{}^{\mathrm{ROV}}\boldsymbol{B}_{\mathrm{JOY}} + {}^{\mathrm{ROV}}\boldsymbol{B}_{\mathrm{LRF}}\right|} & \left(\text{if } \left|{}^{\mathrm{ROV}}\boldsymbol{B}_{\mathrm{JOY}} + {}^{\mathrm{ROV}}\boldsymbol{B}_{\mathrm{LRF}}\right| > 1\right) \end{cases} \tag{11}
$$

However, the upper limit of the collision avoidance behaviour vector ${}^{\mathrm{ROV}}\boldsymbol{B}_{\mathrm{LRF}}$ is set to 50% of the total navigation vector in order to avoid out of control while collision avoidance (Equation 12).

$$
{}^{\mathrm{ROV}}\boldsymbol{B}_{\mathrm{LRF}} = \begin{cases} G \cdot {}^{\mathrm{ROV}}\boldsymbol{A}_{\mathrm{LRF}} & \left(\text{if } \left|G \cdot {}^{\mathrm{ROV}}\boldsymbol{A}_{\mathrm{LRF}}\right| \le 0.5\right) \\ 0.5 \cdot \frac{{}^{\mathrm{ROV}}\boldsymbol{A}_{\mathrm{LRF}}}{\left|{}^{\mathrm{ROV}}\boldsymbol{A}_{\mathrm{LRF}}\right|} & \left(\text{if } \left|G \cdot {}^{\mathrm{ROV}}\boldsymbol{A}_{\mathrm{LRF}}\right| > 0.5\right) \end{cases} \tag{12}
$$

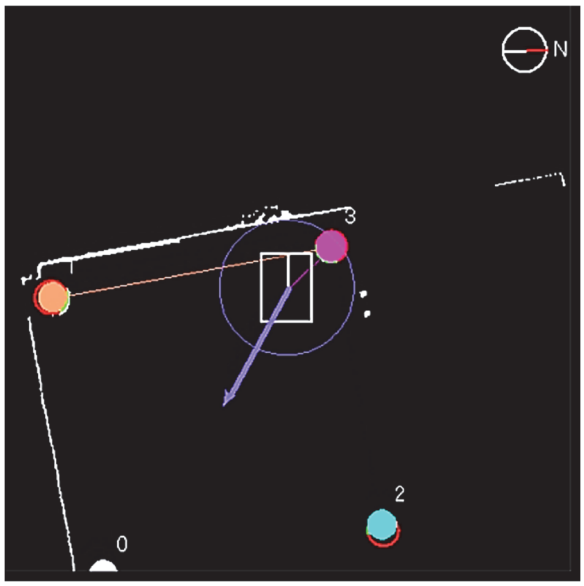

Figure 5. Autonomous collision avoidance behaviour of the ROV

The autonomous collision avoidance behaviour of the ROV is shown in Figure 5. In this figure, the collision avoidance direction has been calculated in response to penetration of the proximate pink pile into the alert-circle-area, and the ROV avoids collision with the pile autonomously.

3.4 Presentation of Shooting History

The picture displayed in the upper part of the in-situ operation application in Figure 3 is the navigation window that displays the ROV on the map database of the piles layout. The operator grasps the current position of the ROV from the information on this window and operates the ROV along the planned inspection route.
The blue line rectangular surrounding the ROV indicates the shooting area of the inspection camera, and the shooting history is presented by leaving the filled shooting area as footprints. In the figure, the filled area in light gray is the captured area. With this function, it is possible to easily distinguish the captured area and the uncaptured area on the underside of the pier superstructure in real time, and it is possible to prevent shooting omissions.

Here, in case of angle of view θ, φ[deg] (horizontal, vertical), shooting distance D[mm], focal length F[mm], sensor size W_s, H_s[mm] (horizontal, vertical), the filled-in area W, H[mm] (horizontal, vertical) as the shooting history in one shooting is expressed multiplying the shooting area of the camera by the safety factor R by Equation (13) [3].

$$
W = 2D \cdot R\tan\theta/2\,,\quad H = 2D \cdot R\tan\varphi/2
$$
$$
\text{where,}\quad \tan\theta/2 = 0.5W_s/F\,,\quad \tan\varphi/2 = 0.5H_s/F \tag{13}
$$

An example of the presentation of the shooting history in field experiment to verify the effect is shown in Figure 6. On the other hand, Figure 7 shows a 3-D model of the pier superstructure constructed by SfM-MVS software from the obtained pictures corresponding to the shooting history.

Both pictures are perspective view looking down the pier superstructure vertically. Comparing shooting history in Figure 6 and the 3-D model in Figure 7, each uncaptured area is the same.

3.5 Effectiveness of Introducing the Developed Technologies

Authors have conducted several field tests for the verification of the developed technologies to date. The proposed method using the technologies is secure and safety because there are no inspectors on the sea.

The proposed method performed well in every test although obtained information were increased. And, one of results showed more than fourfold efficiency on site work to the conventional method by inspectors [4].

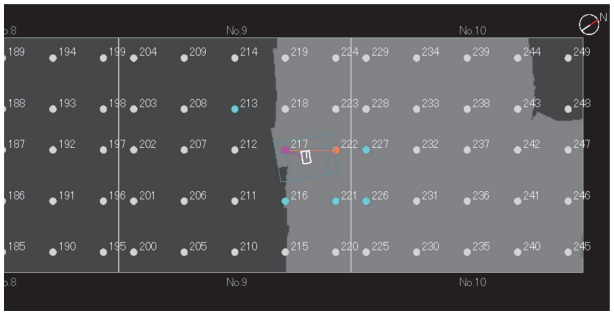

Figure 6. Foot-print of the shooting history

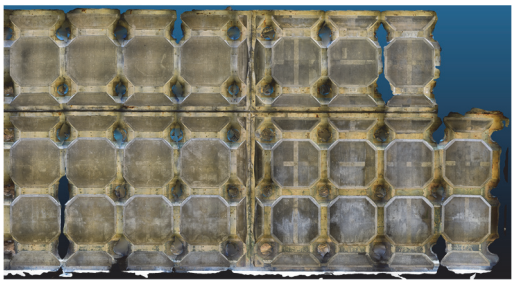

Figure 7. 3-D model concrete pier superstructure constructed by SfM-MVS photogrammetry

4 Inspection and Diagnosis Support System

An inspection and diagnosis support system was also developed for supporting the work to make inspection reports because of obtaining an enormous inspection picture by introduction of the ROV to field work [4][5].

First, 3-D model of the underside of the pier superstructure is composite from obtained pictures using commercially SfM-MVS (Structure from Motion-Multi View Stereo) software. The SfM-MVS technology is a general-purpose technology recently applied to drone photogrammetry and shape measurement of structures.

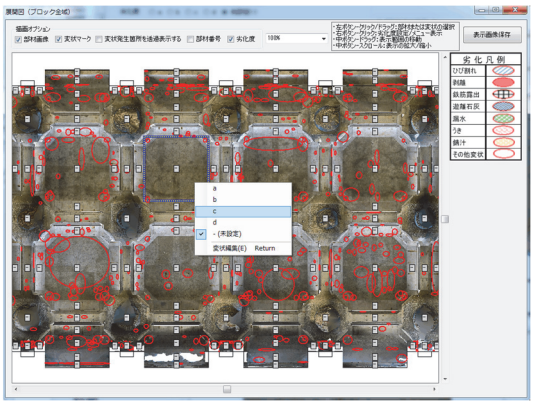

Figure 8. 2-D development view and candidates of suspected deterioration on the support system

2-D development view for each member is automatically created from 3-D model by the inspection and diagnosis support system, and the location that have the possibility of deterioration are automatically detected from the development view in Figure 8. The user distinguishes the position and deterioration type from the detected objects, and classifies the deterioration of the target member as grades a, b, c or d. The inspection report is automatically created based on the distinguished deterioration.

5 Conclusions

This paper reported the ROV for visual inspection of concrete pier superstructure, work support functions for ROV operation, and the inspection and diagnosis support system to save the related work. These are considered to have largely reached a practical level technically

These results promise a certain level of contribution to the improvement of safety and efficiency of the work. Development of linking tool with BIM/CIM is current in progress in order to further improve convenience of them.

Acknowledgements

This work was supported by the Infrastructure Maintenance, Renovation, and Management program of the Cross-Ministerial Strategic Innovation Promotion Program (SIP), which is sponsored by the Council for Science, Technology and Innovation, and funded by the Japan Science & Technology Agency (JST).

References

[1] Tanaka T. et al. Field experiments of positioning and shooting system equipped in inspection vehicle for concrete superstructure of piled pier. In *Proc. the 17th SCR*, O-54, 2017 (in Japanese, USB).

[2] Tanaka T. et al. Enhancement of tele-operation assistance functions of inspection vehicle for concrete superstructure of piled pier. In *Proc. the 18th SCR*, O4-2, 2018 (in Japanese, USB).

[3] Tanaka T. et al. Field test of ROV equipped with tele-operation assistance functions for inspection of concrete pier superstructure. In *Proc. the 19th SCR*, O2-5, 2019 (in Japanese, USB).

[4] Nogami S. et al. Improvement of inspection and diagnosis of concrete pier superstructure by Remotely Operated Vehicle and diagnosis support software. In *Proc. the 74th annual conference of the JSCE*. VI-770, 2019 (in Japanese, DVD-R).

[5] Kato E. et al. Demonstration test for improvement of inspection and diagnosis of concrete pier superstructure by remotely operated vehicle. In *Proc. the 3rd ACF symposium*, S5-3-1, 2019 (USB).